High-resolution animated tectonic reconstruction of the South Pacific and West Antarctic Margin

Article *in* Geochemistry Geophysics Geosystems · July 2004

DOI: 10.1029/2003GC000657

3 authors, including:

Graeme Eagles
Alfred Wegener Institute Helmholtz Centre for Polar and Marine Research
109 PUBLICATIONS **2,951** CITATIONS
SEE PROFILE

Karsten Gohl
Alfred Wegener Institute Helmholtz Centre for Polar and Marine Research
243 PUBLICATIONS **4,618** CITATIONS
SEE PROFILE

Geochemistry Geophysics Geosystems G3
AN ELECTRONIC JOURNAL OF THE EARTH SCIENCES
Published by AGU and the Geochemical Society

Article
Volume 5, Number 7
10 July 2004
Q07002, doi:10.1029/2003GC000657
ISSN: 1525-2027

High-resolution animated tectonic reconstruction of the South Pacific and West Antarctic Margin

Graeme Eagles and Karsten Gohl
Alfred Wegener Institute for Polar and Marine Research, Postfach 120161, D-27515 Bremerhaven, Germany (geagles@awi-bremerhaven.de)

Robert D. Larter
British Antarctic Survey, High Cross, Madingley Road, Cambridge, CB3 0ET, UK

[1] An animated reconstruction shows South Pacific plate kinematics between 90 and 45 Ma, using the satellite-derived gravity anomaly field, interpolated isochrons and plate rotation parameters from both published and new work on marine geophysical data. The Great South Basin and Bounty Trough, New Zealand, are shown as the earliest Pacific–Antarctic plate boundary that opened before 83 Ma. The earliest true Pacific–Antarctic seafloor formed within the eastern parts of this boundary, but later and farther west, seafloor formed within its Antarctic flank. After 80 Ma, the Bellingshausen plate converged with an oceanic part of the Antarctic plate to its east, while its motion simultaneously caused rifting in continental Antarctica to the south. The Pacific–Bellingshausen spreading center developed a set of long offset transform faults that the Pacific–Antarctic plate boundary inherited around chron C27 when the Bellingshausen plate ceased to move independently as part of a Pacific-wide plate tectonic reorganization event. Southwest of these transforms the Pacific–Antarctic Ridge saw an increase in transform-fault segmentation by ~58 Ma. One of the long offset Pacific–Bellingshausen transforms, referred to as "V," was modified during the C27 reorganization event when a Pacific–Antarctic–Phoenix triple junction initiated on its southern edge. Eastern parts of "V" started to operate in the Pacific–Phoenix spreading system, lengthening it even more, while its western parts operated in the Pacific–Antarctic system. This complicated feature was by-passed and deactivated by ridge axis propagation to its northwest at ~47 Ma. We interpret our animation to highlight possible connections between these events.

Components: 11,268 words, 11 figures, 1 table, 1 animation.

Keywords: plate tectonics; plate reconstructions; Pacific Ocean; Antarctica.

Index Terms: 3040 Marine Geology and Geophysics: Plate tectonics (8150, 8155, 8157, 8158); 8157 Tectonophysics: Plate motions—past (3040); 9310 Information Related to Geographic Region: Antarctica.

Received 30 October 2003; **Revised** 23 March 2004; **Accepted** 5 May 2004; **Published** 10 July 2004.

Eagles, G., K. Gohl, and R. D. Larter (2004), High-resolution animated tectonic reconstruction of the South Pacific and West Antarctic Margin, *Geochem. Geophys. Geosyst.*, *5*, Q07002, doi:10.1029/2003GC000657.

1. Introduction

[2] In this paper, we present an animated reconstruction of gridded, satellite-derived free-air gravity data, and use it as a tool to describe the tectonic history of an important region for global tectonics: the South Pacific and its West Antarctic margin. The animation displays events that are described in the literature, as well as some new interpretations, and

it gives a self-consistent view of the region's tectonics.

1.1. Gridded and Animated Reconstructions

[3] Detailed data sets of free-air gravity anomalies, derived from satellite altimetry over the world's oceans [e.g., *McAdoo and Laxon*, 1997; *Sandwell and Smith*, 1997] (Figure 1), illustrate in detail the plate tectonic fabric of the ocean floor, including the fracture zones (FZs) formed at transform faults (TFs), and the traces of triple junction (TJ) migration. Tectonic histories derived from such gridded data are most directly and meaningfully illustrated by reconstruction of the data themselves. Such "state of the art" reconstructions have already been produced for the South Pacific [*Marks and Stock*, 1997; *McAdoo and Laxon*, 1997]. Figure 2 shows that a static reconstruction using gridded gravity data can have the following advantages over a static line drawing (vector) reconstruction: (1) there is a massive increase in the number of reconstructed features, (2) the reconstruction of gridded data is largely free of selection pressure because the choice of "significant" features is confined to the identification of often already well-constrained ancient plate boundaries within which all data are reconstructed, (3) gridded reconstructions explicitly show areas of underlap (compare the Phoenix plate in the two parts of Figure 2; the gray underlap area in the gridded reconstruction clearly shows its destruction at the West Antarctic margin subduction zone, which is not obvious from the vector reconstruction), and (4) reconstructed gridded data are amenable for further quantitative analysis, already in paleocoordinates.

[4] Animated reconstructions are powerful and valuable tools that give viewers a rapid grasp of a tectonic history with which they may be unfamiliar, and a full appreciation of the continuity of plate motion models. They also permit an appreciation of long time series geological data in their paleogeographical context. Like snapshot reconstructions, animated reconstructions can use vector or gridded data.

[5] The PLATES group (http://www.ig.utexas.edu/research/projects/plates/plates.htm#recons), *Reeves and Sahu* [1999] (http://kartoweb.itc.nl/gondwana/), and *Hall* [2002], for example, present animated reconstructions of large volumes of vector data, many digitized from grids, that successfully illustrate global and more detailed regional tectonic models. *Gaina et al.* [1998a, 1998b] (http://www.es.usyd.edu.au/geology/people/staff/dietmar/Movies/tasman.html) present an animated reconstruction of gridded satellite-derived gravity data for the Tasman Sea region. Vector animations have the advantage of lower data volumes, and therefore lower data transfer rates are required to view them, but they suffer some of the same drawbacks as static line drawing reconstructions. In particular, the work associated with digitizing large numbers of features is time consuming and unavoidably involves interpretations and selections that can never fully be documented by the human digitizer. With ongoing increases in computer speed, reconstruction and animation of gridded data becomes both feasible and desirable, and can be achieved with a similar or smaller amount of human effort.

1.2. Tectonic Introduction

[6] The West Antarctic continent (Figure 1) hosts an important example of a continental margin that has changed from an active to a passive setting, and is a crucial yet poorly known link in the Late Cretaceous and Tertiary global plate circuit. The early to mid-Cretaceous proto-Pacific margin of Gondwana was a subduction zone, until Chatham Rise started to separate from it late within the Cretaceous Normal Polarity Superchron (CNS; 118–83 Ma). Subsequently, Campbell Plateau also separated from the Antarctic margin during the reversed part of chron C33 (83–79.1 Ma), leaving a rifted continental margin bordering the Amundsen and westernmost Bellingshausen seas (Figure 1) [*Larter et al.*, 2002]. A spreading center, that was in morphological continuity with the Pacific–Antarctic ridge in the eastern Amundsen Sea, separated a small plate, known as the Bellingshausen plate [*Stock and Molnar*, 1987; *Stock et al.*, 1996], from the Pacific plate until its incorporation into the Antarctic plate around chron C27 (~61 Ma) [*Cande et al.*, 1995]. The "Bellingshausen" parts of the ridge are thought to have been the first to form, before chron C34y (83 Ma), although the Bellingshausen plate probably did not come into existence until shortly afterward [*Eagles et al.*, 2004]. The Bellingshausen plate had slow convergent and divergent margins with Antarctica [*Heinemann et al.*, 1999; *Cunningham et al.*, 2002; *Larter et al.*, 2002]. Further east, the plate facing the West Antarctic

margin was the Phoenix (also called Aluk, or Drake) plate. The Phoenix plate's divergent boundaries with the Pacific, Bellingshausen and Antarctic plates have changed over time [*Cande et al.*, 1982, 1995; *McCarron and Larter*, 1998; *Larter and Barker*, 1991], but its southeastern boundary was continuously a subduction zone where it was being overridden by the Antarctic Peninsula. The Phoenix

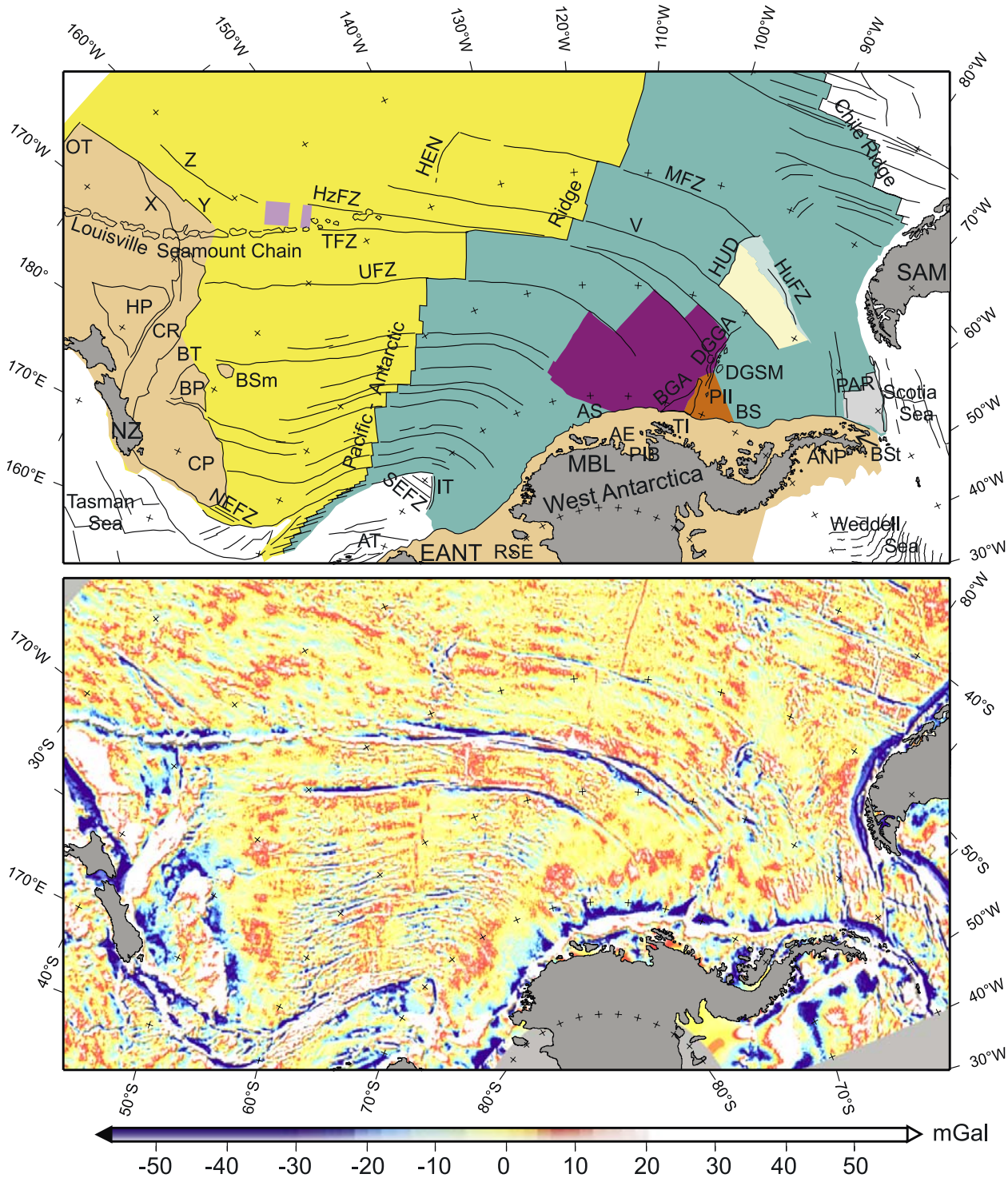

Figure 1

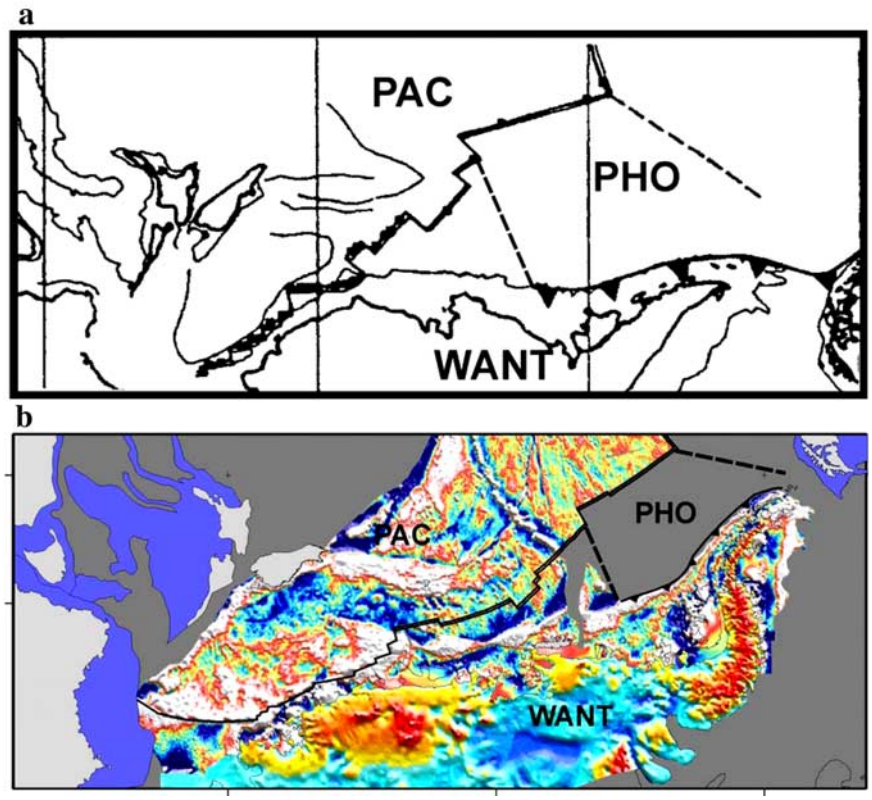

Figure 2. (a) Snapshot line reconstruction of the West Antarctic margin at chron C34y, from *Mayes et al.* [1990]. The label for an Aluk plate has been changed to PHO (Phoenix plate) and that for the Bellingshausen plate has been removed to avoid confusion. (b) Equivalent snapshot gridded free-air gravity reconstruction, with data from the BEDMAP compilation [*Lythe et al.*, 2000] included onshore Antarctica. Graticule interval: 10°. Mercator projection.

plate's later history has seen most of it lost as segments of the Antarctic–Phoenix ridge successively converged with the Antarctic Peninsula from southwest to northeast. This continued until around chron C2A (~3.3 Ma), when the last remnant of the Phoenix plate was incorporated into the Antarctic plate [*Larter and Barker*, 1991; *Livermore et al.*, 2000].

[7] Between the Bellingshausen and Phoenix sectors, a small fragment of the oceanic lithosphere at the margin may have formed on the southern side

Figure 1. (top) Buff, areas already existing at 90 Ma; bright yellow, lithosphere formed on the Pacific plate; bright green, West Antarctic plate; purple, Bellingshausen plate; light yellow, formed on Pacific plate but transferred to Antarctic plate; light green, formed on the Farallon plate and transferred to the Antarctic plate; gray, formed on the Phoenix plate and transferred to the Antarctic plate; light purple, formed on the Bellingshausen plate and transferred to the Pacific plate; orange, formed on the Charcot plate. AE, Amundsen Embayment; ANP, Antarctica Peninsula; AS, Amundsen Sea; AT, Adare Trough; BGA, Bellingshausen Gravity Anomaly; BP, Bounty Platform; BS, Bellingshausen Sea; BSm, Bollons Seamount; BSt, Bransfield Strait; BT, Bounty Trough; CP, Campbell Plateau; CR, Chatham Rise; DGGA, De Gerlache Gravity Anomaly; DGSM, De Gerlache Seamounts; EANT, East Antarctica; HEN, Henry Trough; HUD, Hudson Trough; HP, Hikurangi Plateau; HuFZ, Humboldt FZ; HzFZ, Heezen FZ; IT, Iselin Trough; MBL, Marie Byrd Land; MFZ, Menard FZ; NEFZ, northern parts of Emerald FZs; NZ, New Zealand; OT, Osbourn Trough; PAR, extinct Phoenix–Antarctic ridge; PIB, Pine Island Bay; PII, Peter I Island; RSE, Ross Sea Embayment; SAM, South America; SEFZ, southern parts of Emerald FZs; TI, Thurston Island; TFZ, Tharp FZ; UFZ, Udintsev FZ; V, FZ "V"; and X, Y, Z, gravity lineaments of *Larter et al.* [2002]. Oblique Mercator projection centered on 137.5°W, 65°S and with 74°W, 60°S on the oblique equator. (bottom) Satellite derived free-air gravity anomalies in the study region [*Sandwell and Smith*, 1997; *McAdoo and Laxon*, 1997] (high-pass filtered to remove >1500 km wavelength anomalies and retain those <500 km).

of a CNS-age spreading center between the Pacific plate and the Charcot plate, a fragment of the Phoenix plate. The last remnant of the Charcot plate became fused to the West Antarctic plate when its subduction beneath the West Antarctic margin stalled as part of the plate tectonic reorganization that resulted in formation of the rifted margins further west [*Larter et al.*, 2002].

[8] The West Antarctic subcontinent itself has undergone extension in numerous small basins. Many of these basins are parts of the West Antarctic rift system that started to separate West Antarctica from East Antarctica early in the Tertiary [*Behrendt et al.*, 1991]. Examples of such basins are the Adare Trough, that proceeded to seafloor spreading [e.g., *Cande et al.*, 2000], and basins of the Ross Sea Embayment. Others may be related to local complications to regional tectonics, like Bransfield Strait [e.g., *Barker and Austin*, 1998] and the Powell Basin [*Eagles and Livermore*, 2002].

2. Method

2.1. Finite Rotations

[9] All finite rotations for reconstruction of the various plate pairs are shown in Table 1 and all dates are from the magnetic reversal timescale of *Cande and Kent* [1995]. In some cases, it was necessary to extrapolate parameters in order to generate a 90 Ma finite rotation. These finite rotations were then expressed with respect to a fixed West Antarctica, and interpolated for integer numbers of millions of years between 1 and 90.

[10] *Larter et al.*'s [2002] fit of Chatham Rise to the West Antarctic margin at 90 Ma, an age estimated by extrapolation of spreading rates back to the continental margins NE of the Udintsev FZ, implicitly defines the opening of Bounty Trough. New Zealand's South Island, east of the Alpine Fault, is kept fixed to Chatham Rise. From chron C34y (83 Ma) onward, the Pacific plate is taken to include Chatham Rise, Campbell Plateau, and the Bounty Trough, and the Pacific plate finite rotations are taken from *Cande et al.* [1995], an unpublished manuscript by Joann Stock et al. (from which *Larter et al.* [2002] list some rotations), and *Larter et al.* [2002].

[11] A captured fragment of the Pacific plate exists north of FZ "V" (Figure 1) [*Cande et al.*, 1982]. Its growth and movement prior to capture are calculated by reversing an interpolated Pacific–West Antarctic finite rotation for 47.6 Ma (by which the central and southern parts of the Henry and Hudson ridge propagation scars (Figure 1) are reconstructed to one another) and then adding each of the 61–48 Ma Pacific–West Antarctic finite rotations (the oldest part of the captured fragment formed at chron C27). Thus the fragment is described as fixed to the West Antarctic plate since its capture at 47.6 Ma, and moving at earlier times about Pacific–West Antarctic stage rotations in the West Antarctic reference frame. The part of the captured crust that formed at the Pacific-Farallon ridge is treated similarly, except that we use a 46.7 Ma interpolated Pacific–Antarctic finite rotation to reconstruct the northern parts of the Henry and Hudson troughs.

[12] Most of the Bellingshausen–Pacific finite rotations come from the unpublished manuscript by J. Stock et al. reported by *Larter et al.* [2002]. The rotations' origin is in an inversion of seafloor spreading data using *Chang*'s [1987] implementation of the technique of *Hellinger* [1981]. *Eagles et al.* [2004] report two new rotations in the Bellingshausen sector of the South Pacific, made by visual fitting of FZs and anomalies C34y and C33o as seen in new aeromagnetic data, and use them to demonstrate independent movement of the Bellingshausen plate since around C33o. Movements of fragments of the Bellingshausen plate, captured by the Pacific plate by ridge jumps around anomalies C33 and C32 [*Eagles et al.*, 2004], are described by constructing a Bellingshausen–Pacific–West Antarctic circuit with finite rotations generated from reversed interpolated Bellingshausen–Pacific finite rotations at the times of the modeled ridge-jumps, to which are added finite rotations at older times until the ages of the oldest parts of the two captured fragments.

[13] The Bollons Seamount is treated as having moved in the Pacific–West Antarctic system, but to have been transferred from the Antarctic to the Pacific plate just after 79 Ma [*Sutherland*, 1999; *Eagles et al.*, 2004]. We calculated a new finite rotation to reconstruct the Bollons Seamount to a gap within the reconstructed Campbell Plateau–Antarctica boundary, because using an interpolated 79 Ma Pacific–Antarctic rotation instead resulted in some lateral overlap between the seamount and Campbell Plateau.

[14] The finite rotation parameters for the Phoenix plate come from *Eagles* [2003] for periods since 15 Ma and from an unpublished inversion similar to that reported by *Eagles* [2000] for times before

Table 1. Finite Rotation Parameters Used for the Animation Process[a]

Latitude	Longitude	Angle	Age	Chron	Source
		Pacific Plate With Respect to Bellingshausen Plate			
71.38	−55.57	44.90	61.28	C27	*Cande et al.* [1995]
70.43	−56.55	46.35	63.80	C28r	Stock et al. (unpublished manuscript)
70.88	−51.01	52.48	67.70	C30r	Stock et al. (unpublished manuscript)
71.40	−42.69	59.57	71.50	C32n.1r	Stock et al. (unpublished manuscript)
70.98	−41.28	62.70	73.60	C33y	Stock et al. (unpublished manuscript)
70.57	−34.34	72.30	79.08	C33o	*Eagles et al.* [2004]
		Pacific Plate With Respect to West Antarctic Plate			
64.25	−79.06	0.68	0.39	C1	*Cande et al.* [1995]
67.03	−73.72	2.42	3.58	C2A	*Cande et al.* [1995]
67.91	−77.93	5.42	6.27	C3A	*Cande et al.* [1995]
69.68	−77.06	7.95	9.64	C4A	*Cande et al.* [1995]
71.75	−73.77	10.92	12.82	C5A	*Cande et al.* [1995]
73.68	−69.85	15.17	16.73	C5C	*Cande et al.* [1995]
74.72	−67.28	19.55	24.12	C6C	*Cande et al.* [1995]
74.55	−67.38	22.95	28.75	C10	*Cande et al.* [1995]
74.38	−64.74	27.34	33.55	C13	*Cande et al.* [1995]
74.90	−51.31	34.54	43.79	C20	*Cande et al.* [1995]
74.52	−50.19	37.64	47.91	C21	*Cande et al.* [1995]
73.62	−52.50	40.03	53.35	C24	*Cande et al.* [1995]
71.38	−55.57	44.90	61.28	C27	*Cande et al.* [1995]
70.55	−55.72	47.00	63.80	C28r	Stock et al. (unpublished manuscript)
68.94	−55.52	49.60	67.74	C30r	Stock et al. (unpublished manuscript)
69.33	−53.44	51.05	68.74	C31	*Cande et al.* [1995]
67.10	−57.40	50.48	71.50	C32n.1r	Stock et al. (unpublished manuscript)
66.72	−55.04	53.74	73.62	C33y	Stock et al. (unpublished manuscript)
		Campbell Plateau With Respect to West Antarctic Plate			
65.58	−52.38	63.07	83.00	C34y	*Larter et al.* [2002]
		Chatham Rise With Respect To West Antarctic Plate			
64.06	−49.94	67.99	90.00	FIT	*Larter et al.* [2002]
		Bollons Seamount With Respect to West Antarctic Plate			
66.28	−54.36	58.52	79.00	FIT	this study
		Pacific Plate With Respect to Hot Spots			
72.000	−80.000	21.000	23.6	Not given	*Yan and Kroenke* [1993]
69.446	−73.652	25.553	30.8	Not given	*Yan and Kroenke* [1993]
67.742	−66.178	33.386	43.0	Not given	*Yan and Kroenke* [1993]
52.375	−79.290	42.427	65.0	Not given	*Yan and Kroenke* [1993]
47.507	−80.108	48.900	74.0	Not given	*Yan and Kroenke* [1993]
		Phoenix Plate With Respect To West Antarctic Plate			
−68.07	−91.96	1.83	5.23	C3	*Eagles* [2003]
−69.21	−97.32	3.07	6.57	C3A	*Eagles* [2003]
−68.98	−90.41	5.85	8.07	C4	*Eagles* [2003]
−69.77	−92.17	7.94	9.31	C4A	*Eagles* [2003]
−69.98	−94.12	11.23	10.95	C5	*Eagles* [2003]
−70.23	−96.68	13.38	12.40	C5A2	*Eagles* [2003]
−70.02	−94.97	18.94	14.61	C5AD	*Eagles* [2003]
−70.03	−79.68	20.75	16.73	C5C	Eagles (unpublished data)
−70.64	−71.93	22.08	20.13	C6	Eagles (unpublished data)
		East Antarctic Plate With Respect to West Antarctic Plate			
−18.15	−17.85	−0.7	33.55	C13	*Cande et al.* [2000]
−18.15	−17.85	−1.7	43.79	C20	*Cande et al.* [2000]
−18.15	−17.85	−1.7	53.3	C24o	*Cande and Stock* [2004]
−18.15	−17.85	−2.2	61.1	C27	*Cande and Stock* [2004]

Table 1. (continued)

Latitude	Longitude	Angle	Age	Chron	Source
		South America Plate With Respect to East Antarctic Plate			
81.80	−33.55	0.63	2.58	C2Ay	*Nankivell* [1997]
81.63	−17.17	2.57	9.74	C5y	*Nankivell* [1997]
79.15	−17.17	5.53	19.05	C6y	*Nankivell* [1997]
75.38	−12.33	7.67	25.82	C8y	*Nankivell* [1997]
74.98	−4.31	10.13	33.06	C13y	*Nankivell* [1997]
76.47	1.81	12.09	38.43	C18y	*Nankivell* [1997]
77.55	10.52	13.66	42.54	C20y	*Nankivell* [1997]
78.14	11.80	14.74	46.26	C21y	*Nankivell* [1997]
79.30	59.56	22.54	65.58	C30y	*Nankivell* [1997]
77.78	53.96	23.92	71.07	C32y	*Nankivell* [1997]
77.73	55.63	25.22	73.62	C33y	*Nankivell* [1997]
77.61	61.48	27.81	79.08	C33Ry	*Nankivell* [1997]
77.36	64.44	29.64	83.00	C34y	*Nankivell* [1997]
		Lord Howe Rise/Challenger Plateau With Respect to Australia			
−14.19	−49.59	0.723	53.3	C24o	*Gaina et al.* [1998a]
−15.93	−46.53	2.112	55.8	C25y	*Gaina et al.* [1998a]
−16.93	−43.77	3.792	57.9	C26o	*Gaina et al.* [1998a]
−4.65	−48.49	4.432	61.2	C27o	*Gaina et al.* [1998a]
−4.71	−47.32	5.168	62.5	C28y	*Gaina et al.* [1998a]
−0.19	−49.63	5.461	64.0	C29y	*Gaina et al.* [1998a]
−3.99	−48.20	6.735	65.6	C30y	*Gaina et al.* [1998a]
−9.04	−45.54	8.83	67.7	C31y	*Gaina et al.* [1998a]
−9.53	−42.8	12.937	73.6	C33y	*Gaina et al.* [1998a]
4.5	−42.26	16.61	90.00	FIT	*Gaina et al.* [1998a]
		East Antarctica With Respect to Australia			
13.45	33.92	20.52	33.6	C13o	*Royer and Rollet* [1997]
14.32	31.75	23.77	40.1	C18o	*Royer and Rollet* [1997]
15.07	31.78	24.55	43.0	C20o	*Tikku and Cande* [2000]
14.00	33.34	24.70	46.0	C21y	*Tikku and Cande* [2000]
10.39	35.59	25.15	53.0	C24o	*Tikku and Cande* [2000]
9.95	36.52	25.55	61.0	C27y	*Tikku and Cande* [2000]
9.48	37.02	26.13	71.0	C32y	*Tikku and Cande* [2000]
5.13	39.80	26.57	79.0	C33o	*Tikku and Cande* [2000]
2.05	40.79	27.12	83.0	FIT	*Tikku and Cande* [2000]
		Eastern South Tasman Rise With Respect to Australia			
−48.23	133.46	0.17	65.6	C30y	*Royer and Rollet* [1997]
−48.23	133.46	2.47	73.6	C33y	*Royer and Rollet* [1997]
−48.23	133.46	5.17	83.0	C34y	*Royer and Rollet* [1997]
−48.23	133.46	8.62	95.0	FIT	*Royer and Rollet* [1997]

[a] Where parameters are quoted from cited references, the precisions used are as given in those references except those from the unpublished Stock et al. manuscript, which are quoted as by *Larter et al.* [2002]. All the rotations are right-handed.

then. We use total reconstruction rotations for the Pacific plate with respect to the hot spots [*Yan and Kroenke*, 1993], in a circuit with *Cande et al.*'s [1995] parameters, to generate parameters for movements between the Louisville hot spot and the West Antarctic plate. We estimated the present-day position of the hot spot, whose trace since ~12 Ma is not obvious [*Wessel and Kroenke*, 1997], by using these parameters to project dated seamounts of the Louisville ridge [*Watts et al.*, 1988] forward in time. The estimated present-day position of the hot spot (134.9°W, 51.5°S) was then rotated by the Hot spots–West Antarctica rotations to give the Louisville hot spot's position for every 1 m.y. interval since 90 Ma.

[15] We use finite rotations for movements between East Antarctica and South America [*Nankivell*, 1997], Australia [*Tikku and Cande*, 2000], the eastern South Tasman Rise [*Royer and Rollet*, 1997] and Challenger Plateau/central Lord Howe Rise [*Gaina et al.*, 1998a] in order to place the gridded animation in its paleogeographical context. These plate movements must be adjusted

in order to take account of what is known of post-90 Ma movements between East and West Antarctica and in New Zealand. However, reconstructions of the Ross Sea region are the subject of controversy, and in view of the lack of consensus on a set of finite rotations there, we have restricted the gridded data reconstruction to those plates linked to West Antarctica via a circuit of long spreading ridge plate boundaries. Outside this circuit, movements are shown simply using outlines defined from free-air gravity data, and present-day coastlines.

[16] For the adjustment of these movements, East–West Antarctica rotations are taken from *Cande et al.* [2000] and *Cande and Stock* [2004], who describe movements in the Adare Trough and basins in the Ross Sea Embayment between chrons C20 and C8, and between chrons C27 and C24. We do not use the finite rotation of *Marks and Stock* [1997] (derived from closure of the Iselin Trough and alignment of the Emerald FZs) because this implies convergence, not divergence, between East and West Antarctica between C27 and C24. This rotation may instead only apply to a microplate that bore the Iselin Bank. The finite rotations we use are based on the closure of reconstruction misfits on short lengths of oceanic plate boundaries, and hence are not tightly constrained. Nonetheless, when combined with *Cande et al.*'s [1995] and *Tikku and Cande*'s [2000] rotations, they do produce a finite rotation for reconstruction of the Emerald basin that is within the estimated uncertainties of a finite rotation [*Sutherland*, 1995] derived from reconstruction of the margins of that basin. Although *Wood et al.* [2000] show that southwestern parts of New Zealand were tectonically quiet between Late Cretaceous rifting in the Tasman Sea and Eocene opening of the Emerald Basin, it is not possible to rule out pre-C27 movements in New Zealand or between East and West Antarctica. For simplicity, prior to C27, we fix East Antarctica and West Antarctica together and leave the boundary within New Zealand free.

[17] Finally, some small basin opening events within West Antarctica (e.g., Bransfield Strait and Powell Basin) are not shown as part of the animation.

2.2. Generating the Animation: Assumptions, Method, and Limitations

[18] Our animation uses many reconstruction parameters derived from inversions of magnetic isochron and FZ data, and so is obliged to illustrate the consequences of the assumptions of the inversions. These inverse techniques may omit information from FZs formed at long offset (>200 km) TFs, either on the assumption that they do not behave passively in changing kinematic settings [e.g., *Shaw and Cande*, 1990] or for reasons of technical unsuitability [*Hellinger*, 1981]. There are observations to support the assumption that some long offset TFs do not behave passively [*Cande et al.*, 1988; *Müller and Roest*, 1992]. An opposing opinion holds that FZs from long offset TFs are the most reliable indicators of plate motion because they exert a strong influence on it. In this view, shorter offset TFs are more likely to behave nonpassively. If, instead, we had chosen to illustrate reconstructions that favor long offset FZ data (e.g., the visual fit-derived reconstructions of *Mayes et al.* [1990]) our animation would have been constrained to illustrate the migratory responses of short-offset TFs to plate motion changes.

[19] To generate the animation, we digitized a set of 471 masks covering whole plates or parts of plates (Figure 3). These masks show the outlines of surviving crust of single plates, at 1 m.y. intervals, between 90 and 1 Ma. The masks parallel the nearest known magnetic anomaly isochrons [*Cande et al.*, 1989] and are offset along FZs interpreted from the gravity data. Where there are no magnetic anomaly data, or their azimuths are poorly-constrained, we generate synthetic age points using interpolated finite rotations to grow synthetic flow lines from seed-points of known age, and assume that isochrons through these points strike normal to the FZs.

[20] It is important to remember that interpolation of isochrons and rotations is sensitive to dating and magnetic timescale errors. Interpolation is also sensitive to some assumptions made implicitly when interpolating rotations and isochrons: firstly that seafloor spreading was continuous, and secondly that it was symmetrical about and, thirdly, perpendicular to, ridge crest segments. The assumption of continuity is reasonable because the reconstruction anomalies used are in quite short time steps, and their rotation parameters define synthetic FZs that are good matches to real ones in gravity data. However, for interpolation of magnetic isochrons, the assumption of symmetrical spreading is often less than reasonable and, if the interpolated stage

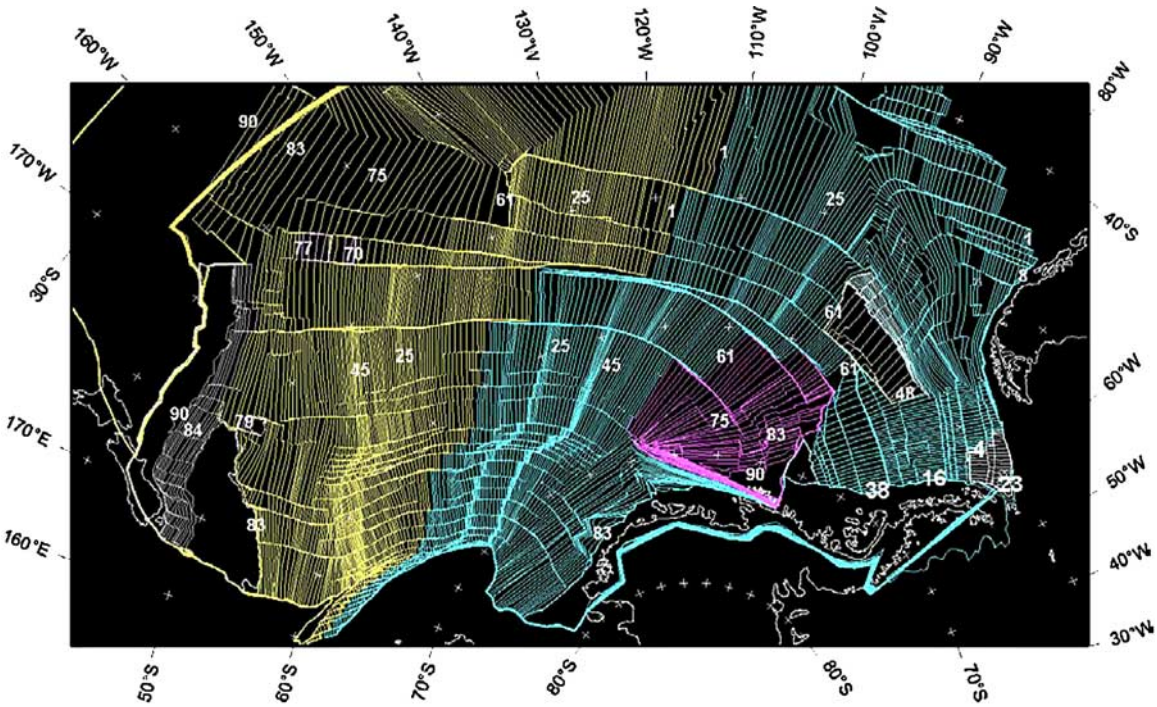

Figure 3. Plate masks on which the animation is based. Yellow, Pacific plate; blue, (West) Antarctic plate; mauve, Bellingshausen plate; light yellow, formed on Pacific plate but transferred to Antarctic plate; light blue, formed on the Farallon plate and transferred to the Antarctic plate; lilac, formed on the Bellingshausen plate and transferred to the Pacific plate; gray, formed on the Phoenix plate and transferred to the Antarctic plate (also Campbell Plateau, Chatham Rise, and Bollons Seamount masks). Numbers indicate the age of the masks (in Ma). Projection as in Figure 1.

is a long one, it could introduce significant inaccuracy into the animation. Oblique spreading is uncommon, and its presence can be tested for, crudely, by comparing the free-air anomaly grid, that often shows an isochron-parallel fabric, to the digitized masks.

[21] The finished masks are the framework for a set of ninety grid files of rotated data that are used to illustrate the steps in the animation. First, each mask is used to extract data from a composite grid file of Bellingshausen Sea and South Pacific free-air gravity anomalies [*Sandwell and Smith*, 1997; *McAdoo and Laxon*, 1997]. The grid file is generated simply, by adding over complementary amplitude ramps in the regions where the two published grids overlap. Any other grid file of suitable extent could, of course, be used. The extracted data are reformatted, rotated, and reregistered to new geographic grids using a combination of GMT [*Wessel and Smith*, 1998] and purpose-written FORTRAN routines and shell scripts.

[22] The reconstructed grid files are used as the bases of color frames for animation. Onshore in West Antarctica, the only significant region of land in the reconstructed region, we substitute the BEDMAP subice topography data set [*Lythe et al.*, 2000]. Selected land areas, mask outlines (to define the reconstructed plate boundaries) and isochron data from *Cande et al.* [1989] are reconstructed with the same set of rotation parameters and overlaid. The isochron data should coincide with the rotated masks at the divergent plate boundaries for reconstruction times that are near to the ages of mapped reversal anomalies. In fact, this is not always the case because our interpretation of divergent boundary segmentation is based on the free-air anomaly expression of FZs, but the compilation of magnetic anomaly isochrons we use [*Cande et al.*, 1989] is often based on sources that predate the widespread use of satellite altimetry data. An updated compilation of magnetic anomaly isochrons for the region that is also compatible with the segmentation evident from FZs in satellite

free-air gravity would improve the usefulness of isochron data overlaid on the grid reconstructions in the individual frames.

3. Results

[23] Animation 1 shows the parts of the animation covering the times discussed in this section (90–45 Ma). Animation 1 shows a "traffic light" symbol in its top-right corner that shows red in frames where finite rotations for the gridded part of the reconstruction are interpolated, amber where they are estimated from fits of continental outlines, and green where they are based on fits of both magnetic isochrons and FZ data. Below, we describe Animation 1 with reference to figures showing still frames from important epochs. The figures are annotated in order to enable readers to refer more easily to the text, whereas the equivalent frames in the animation are not. We present the frames from oldest first to youngest last, but it should be remembered that the two oldest reconstructions (90 and 83 Ma) are more speculative than the younger ones, because they are based on rather less well-constrained rotations based on seafloor fabric and visual fits of the continental margins.

3.1. Earliest Movements: 90-83 Ma

[24] The 90 Ma "complete fit" reconstruction in Figure 4 is based closely on that of *Larter et al.* [2002], and can be compared to that of *Sutherland* [1999]. The Osbourn Trough (OT) lies in the far north of the reconstructions. Although *Billen and Stock* [2000] proposed that OT was a spreading center that ceased activity at ~72 Ma, this was based on magnetic anomaly profiles that were too short to be unequivocal, and is not consistent with the effective elastic thickness of the lithosphere calculated from the loading effect of nearby seamounts of the Louisville chain [*Watts et al.*, 1988]. *Lonsdale* [1997] and *Larter et al.* [2002] suggest instead that OT was part of the Pacific–Phoenix ridge that stopped spreading at ~105 Ma, based on regional palaeomagnetic, geological and plate kinematic considerations. To the south, the Hikurangi Plateau, which is likely to be a thickened oceanic crustal igneous province, is juxtaposed today with Chatham Rise, which may indicate that a collision between them was responsible for extinction of OT [*Mortimer and Parkinson*, 1996]. Such an event would have accreted the Phoenix plate ocean floor south of OT to the Antarctic plate and, subsequently, necessitated a single new Pacific–Antarctic plate boundary to replace the Pacific–Phoenix boundary at OT and the Phoenix–Antarctic subduction zone. This plate boundary could have taken the form of extension of Zealandia, in the manner first suggested by *Luyendyk* [1995], and we show it as the opening of Bounty Trough and the Great South Basin. This depiction is broadly consistent with the subsidence and depositional history of the Great South Basin [*Carter*, 1988; *Cook et al.*, 1999] and with studies of Bounty Trough [*Davy*, 1993; *Cook et al.*, 1999]. Current work in western and central Bounty Trough is investigating whether seafloor spreading occurred there [*Gohl*, 2003].

[25] The animation shows simple southward convergence of the Charcot plate with the Antarctic margin in the period 90–84 Ma [*Larter et al.*, 2002]. Three gravity anomaly lineations, that *Larter et al.* [2002] termed X, Y, and Z and discussed in the context of the Charcot plate, are labeled, although we do not show anomaly X as a ridge-trench TF as those authors did. The Charcot plate's convergence is illustrative only in the absence of reliable indicators of relative movements, but it highlights the possible existence of a long ridge-trench TF along the plate's western edge. This TF, along which gravity anomaly Y may have formed, was later the location of convergence at the BGA [*Larter et al.*, 2002]. The setting of the Charcot plate fragment thus echoes that of the Phoenix plate fragment that is now welded to the Antarctic plate in Drake Passage [*Larter and Barker*, 1991], and present-day convergent motions across the Shackleton FZ [*Thomas et al.*, 2003] make it a useful analogue to the embryonic BGA. If *Lonsdale* [1997] and *Larter et al.* [2002] are correct in their assessment of OT as part of the Pacific–Phoenix ridge, then we can surmise that the Charcot plate must have converged more rapidly with the Antarctic plate than the Phoenix plate did, because of the subsequent development of gravity anomaly Z and its left-handed offset of anomaly C34y.

[26] The 83 Ma (~C34y) frame is shown in Figure 5. This reconstruction is also based on one of *Larter et al.*'s [2002] reconstructions, and can be compared to that of *Mayes et al.* [1990]. *Larter et al.* [2002] suggest that it is possible the timing of breakup was influenced by propagation of the Charcot–Pacific ridge into the gently extending Zealandia region. Hence we show the Pacific–Antarctic ridge as first becoming active in this frame, when extension in the Bounty Trough and Great South Basin ends. Western parts of the

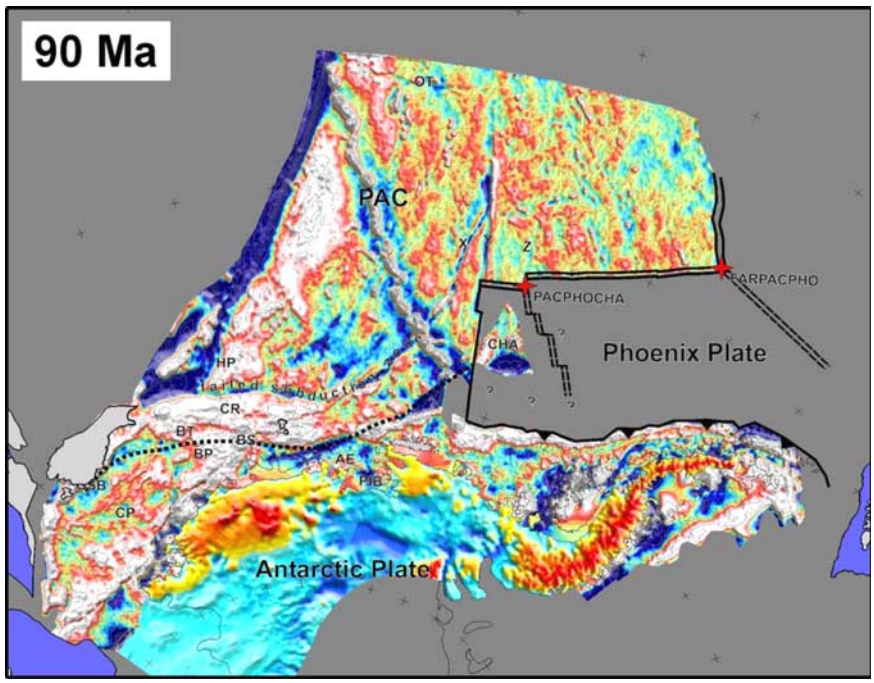

Figure 4. Animation frame for 90 Ma. Red four-point star, TJ; blue fill, continental blocks (defined from satellite-free-air gravity); gray fill, simplified present-day coastlines not in the West Antarctic plate subcircuit (see text). BEDMAP data onshore Antarctica, as in Figure 2; no attempt has been made to define the later plate boundary between West and East Antarctica. Labels as in Figure 1 plus CHA, surviving fragment of Charcot plate; FAR, Farallon; PAC, Pacific plate; PHO, Phoenix. Projection as in Figure 1, graticule interval 10°.

Pacific–Antarctic ridge are only just about to form between the Campbell Plateau and Marie Byrd Land, ~400 km inside the Antarctic flank of the older Bounty Trough/Great South Basin margin. We show the changeover as a simple jump of the entire locus of extension at 83 Ma, but a diachronous changeover could explain the lineament between the Bounty Platform and Campbell Plateau as a short-lived continental transform (dashed line in Figure 5).

[27] In both Figures 4 and 5, Bounty Trough, the Amundsen Embayment's coast, Pine Island Bay and the subglacial beneath Pine Island Glacier can be seen to be colinear features that approximate small circles about a pole nearby to the south. Hence it may be that these features are all lengths of a continental strike-slip zone (a rift zone would follow a great circle trend) that predated extension in the Bounty Trough region. This hypothetical strike-slip zone could be related to strain partitioning in response to oblique subduction or to a much older structure.

3.2. Seafloor Spreading: 83-76 Ma

[28] The 76 Ma (mid-chron C33) frame is shown in Figure 6. *Larter et al.* [2002] suggest the onset of independent movement of the Bellingshausen plate shortly after this time, at about 74 Ma, based on a change in strike of the Udintsev FZ, and two FZs northeast of it. However, *Eagles et al.* [2004] demonstrate Bellingshausen plate movement for times before 74 Ma, and relate these changes in FZ strike to the appearance of the long offset Tharp FZ on the Bellingshausen–Pacific ridge at this time. Hence a Bellingshausen plate is shown with an eastern boundary running through the Bellingshausen Gravity Anomaly (BGA). The plate's southern boundary is more speculatively located, on the bases of its possible identification in seismic reflection data near the Antipodes FZ [*Heinemann et al.*, 1999] and that post-C33y Bellingshausen–Antarctic movements appear to close Peacock Sound tightly [*Larter et al.*, 2002]. The boundary may instead have been confined to the oceanic crust north of Thurston Island (as considered by *Stock et al.* [1996]), or have occurred further into the Antarctic continent [*Larter et al.*, 2002].

[29] The Heezen TF has an offset of ~200 km, which starts to appear in the animation after 80 Ma. Anomaly Z fades out in the region just north of the Heezen and Tharp FZs. *Watts et al.* [1988] and *Larter et al.* [2002] show Z as the trace of a TJ

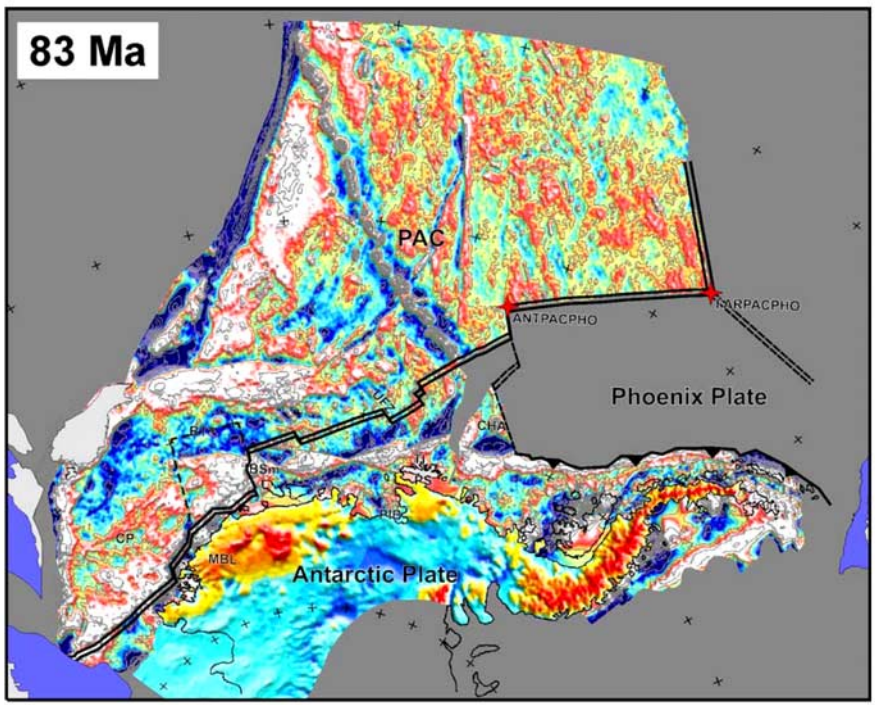

Figure 5. Animation frame for 83 Ma. Projection, graticule, symbols, and labels as for Figures 1 and 4.

between the Pacific, Phoenix and a third plate. *Eagles et al.* [2004] use magnetic anomaly profiles to show how the TJ migrated along a transfrom at Z and into the region now occupied by the Heezen FZ, and how this transform changed its offset sense and started to lengthen at about 80 Ma. They suggest that independent motion of the Bellingshausen plate was related to the appearance of long offset TFs in response to this change. Hence, in this frame (76 Ma), the third plate is the Bellingshausen plate, and the Heezen TF is growing between a northeastern fast spreading Pacific–Phoenix ridge segment and a slower southwestern Pacific–Bellingshausen one.

[30] A Phoenix–Bellingshausen–Antarctic TJ lies not far south of this TJ. The Bellingshausen–Phoenix plate boundary would have been very short at this stage and, by composition of a Bellingshausen–Pacific–Phoenix circuit for the stage C34y–C27o (Figure 7a), is likely to have been divergent [*McCarron and Larter*, 1998] (Figure 7b). The Phoenix–Bellingshausen–Antarctic TJ falls near the north end of a triangular region of underlap between the Bellingshausen plate and the captured Charcot fragment of the Antarctic plate [*Larter et al.*, 2002]. This triangular region represents surface area that no longer exists at the present-day—parts of Bellingshausen plate lithosphere that were compressed and thrust beneath the Antarctic plate. *Gohl et al.* [1997] and *Cunningham et al.* [2002] identified the BGA as a buried inactive compressional zone from seismic reflection data and gravity data modeling: it is the "trench" arm of the TJ. The animation shows ~200 km of horizontal shortening at the northern BGA, decreasing southward to zero southeast of Thurston Island near where the contemporary Bellingshausen–Antarctic stage pole lies, after this frame.

[31] The frame shows a third TJ, the Bellingshausen–Pacific–Antarctic triple junction, in the region of the Marie Byrd seamounts as ridge–ridge–ridge type, although the Bellingshausen–Antarctic arm may not have undergone true seafloor spreading due to its very slow divergence rate. *Heinemann et al.* [1999] identified buried topography in the region that they interpreted as a crossing of the Bellingshausen–Antarctic plate boundary graben, but this could also be interpreted as the TJ trace formed by the presence of a slow spreading arm on a ridge–ridge–ridge triple junction [*Mitchell and Parson*, 1993].

3.3. Seafloor Spreading: 76-68 Ma

[32] The 68 Ma (mid-chron C31) frame is shown in Figure 8. The triangular underlap to the east of the BGA has been greatly reduced by active conver-

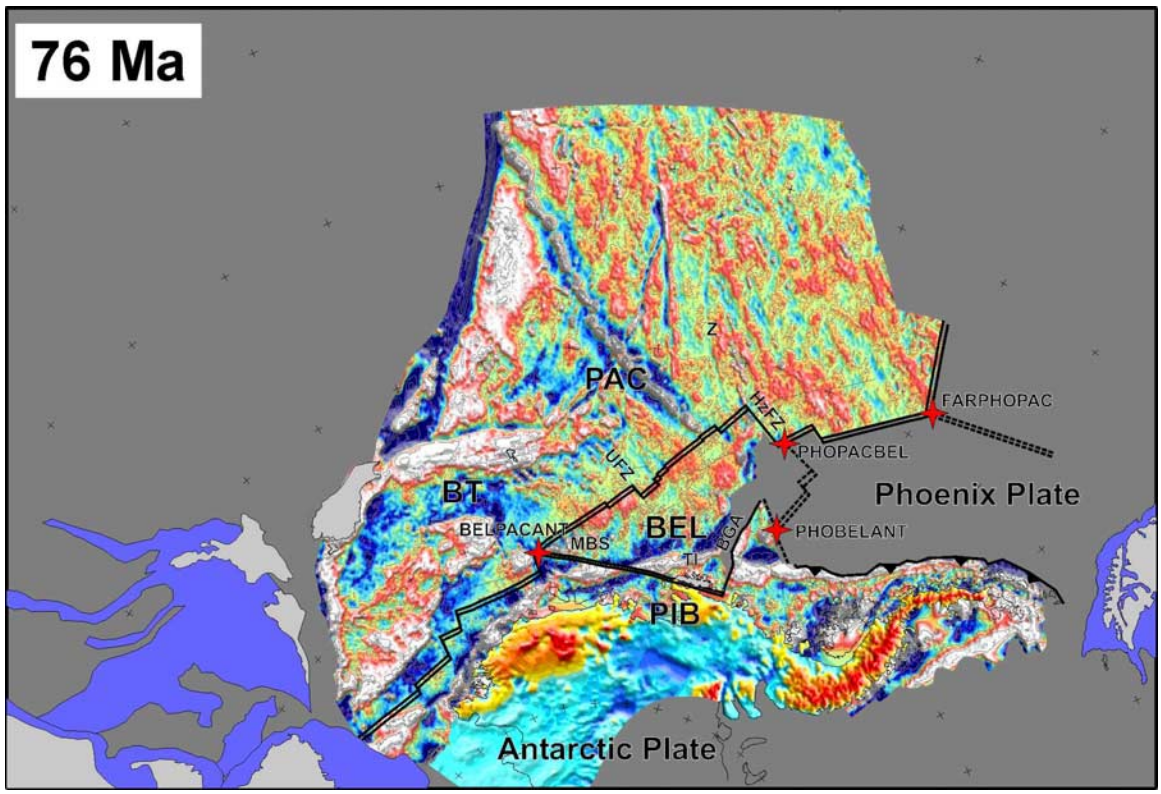

Figure 6. Animation frame for 76 Ma. Projection, graticule, symbols, and labels as for Figures 1 and 4 plus BEL, Bellingshausen plate; MBS, Marie Byrd Seamounts.

gence since the preceding (76 Ma) frame. This convergence occurs as a consequence of rotation of the Bellingshausen plate, relative to the Antarctic plate before chron C31, about stage poles nearby to its SE. The rotation is appropriate, as it corrects the FZ misfits presented by *McAdoo and Laxon*'s [1997] gridded reconstruction as evidence for Bellingshausen plate motion. We show continued rifting at the Bellingshausen–Antarctic boundary in Peacock Sound.

[33] In this frame, the Tharp TF can be seen to have an offset of ~250 km, in contrast to a much shorter offset before. The animation shows this offset to be the result of SE-directed jumps of the Pacific–Bellingshausen ridge at ~74 and ~70 Ma [*Eagles et al.*, 2004]. These events transferred large parts of the Bellingshausen plate to the Pacific plate. The Heezen TF simultaneously shortens due to each of these jumps, but immediately after each it resumes lengthening because it continues to host the Phoenix–Pacific–Bellingshausen TJ. The ridge jumps might have been a response to increasing stress on the lengthening Heezen TF arm of the TJ, which probably had an unstable geometry.

[34] The Udintsev TF is also lengthening in this frame, and does so between 74 Ma and 65 Ma, in response to along-strike variations in spreading asymmetry at the Bellingshausen–Pacific spreading center [*Stock et al.*, 1996; *Larter et al.*, 2002]. This lengthening accompanies that of the Heezen TF that hosted the Phoenix–Pacific–Bellingshausen TJ, and immediately follows the introduction of the Tharp TF into the Bellingshausen–Pacific spreading center by a ridge jump.

[35] There is no known evidence north of the BGA for shortening between the Bellingshausen and Antarctic plates. The Phoenix–Bellingshausen–Antarctic TJ could instead have existed to the southeast in the now-subducted region east of the captured Charcot fragment, perhaps migrating, as shown, along a transform on its NE facing edge and possibly even as far as the subduction zone at the Antarctic margin.

3.4. Seafloor Spreading: 68-61 Ma

[36] Figure 9 shows the reconstruction frame for 61 Ma (near the end of chron C27). The Bellingshausen plate is shown to have ceased independent motion as part of a suite of changes that occurred

around Antarctica at about that time that may have included, or was shortly followed by, the onset of movements between East and West Antarctica [*Cande et al.*, 1995; *Müller et al.*, 2000; *Cande and Stock*, 2004]. Hence the underlap on the BGA no longer exists and no Bellingshausen plate boundaries are shown.

[37] The De Gerlache Gravity Anomaly (DGGA) extends north of the BGA as far as FZ "V". *Larter et al.* [1999] show how magnetic anomaly patterns suggest that the DGGA represents a scar from initiation of an Antarctic–Phoenix ridge after extinction of the Bellingshausen plate during the chron C27 tectonic reorganization. We show this new Antarctic–Phoenix ridge, with its crest geometry based on later isochron offsets east of the DGGA. In the previous sections, we noted the presence of the Pacific–Phoenix–Bellingshausen TJ, and its traces, in the region to the north of the BGA, and here we suggest that one of these traces may have formed a suitable target for the initiation of the new plate boundary there. *Gohl et al.* [1997] propose that this line was influential yet again later, as the DGGA formed a sublithospheric channel or upwelling locus for Miocene volcanism at Peter I Island [*Prestvik and Duncan*, 1991] and the De Gerlache Seamounts [*Hagen et al.*, 1998].

[38] The animation shows that the Heezen TF stops lengthening and, north of it, the TF on "V" starts lengthening, at ~64 Ma (young end of chron C29). These observations are subject to the correctness of the picks in *Cande et al.*'s [1989] compilation that come from *Cande et al.* [1982]. These workers interpret the observations to indicate northward movement of the Phoenix–Pacific–Bellingshausen TJ from the Heezen TF to TF "V" at 64 Ma. The Heezen TF thus acted as a simple, long offset, Bellingshausen–Pacific ridge transform after 64 Ma.

[39] Figure 9 shows the backtracked Louisville hot spot, as a red five-pointed star, that first appears in the animation at 73 Ma. The hot spot moves SE with respect to the Pacific plate during the course of the animation, tracking the line of free-air anomalies associated with the Louisville seamount chain. Where a located seamount's age is known, the animation shows it as an orange triangle symbol (as in Figure 9). The animation frames show all the gravity anomalies associated with seamounts on crust older than their age, rather than all those older than the age of the frame. It must be remembered that the "seamount" gravity anomalies SE of the hot spot are most likely not to have existed at the time of the frame being viewed. This failing is one area in which future versions of the animation could be significantly improved.

3.5. Seafloor Spreading: 61-55 Ma

[40] The 55 Ma (chron C24n.3) frame is shown in Figure 10. "V" finds itself in a new setting after the events at around C27. The West Antarctic–Pacific–Phoenix TJ, at the northern tip of the new Antarctic–Phoenix ridge along the DGGA, migrated ESE along "V" from about 91.5°W, 58.8°S. "V" hence underwent a diachronous transition between two settings: east of the TJ it operated in the Phoenix–Pacific system, but west of the TJ it was the site of a new West Antarctic–Pacific plate boundary. "V" was also lengthening all the time due to the spreading rate difference between the Pacific–Antarctic and Pacific–Phoenix ridges at its NW and SE ends, respectively. The nature of the West Antarctic–Pacific boundary on "V" is difficult to predict because it is difficult to define its preexisting trace as a Phoenix–Pacific feature due to complicated free-air anomalies and sparse magnetic anomaly data east of the DGGA. We illustrate a situation in which the Antarctic–Phoenix ridge tip propagates northward to stay in contact with a TJ migrating along a "V" drawn through one of the northernmost free-air anomaly troughs in the area, which retains a strike-slip character. We interpret the SE-trending free-air anomaly troughs to the south of this as FZs formed on the Antarctic–Phoenix ridge. If we had chosen to draw "V" in a more southerly position, then we could interpret the free-air anomaly features as rugged topography formed at, or north of, a reactivated transpressional "V".

[41] Following chron C27, Pacific–West Antarctic spreading gradually rotated into a slightly more WNW azimuth than its previous NW one, and a substantial drop in spreading rate is demonstrable from finite rotations between C27 and C25/C24 [*Mayes et al.*, 1990; *Cande et al.*, 1995]. Our animation shows the Pacific–Antarctic ridge's responses to these changes. In the SW sector of the ridge, the previous set of 4 medium or short offset, mostly left-stepping TFs is replaced by 2–3 times as many short offset, right-stepping TFs, as noted by *Cande et al.* [1995]. In drawing our masks, we have assumed that the process involved was symmetrical and involved simultaneous ridge crest subsegmentation and rotation of the subsegments. If these assumptions are correct, the animation suggests the TF population increase was

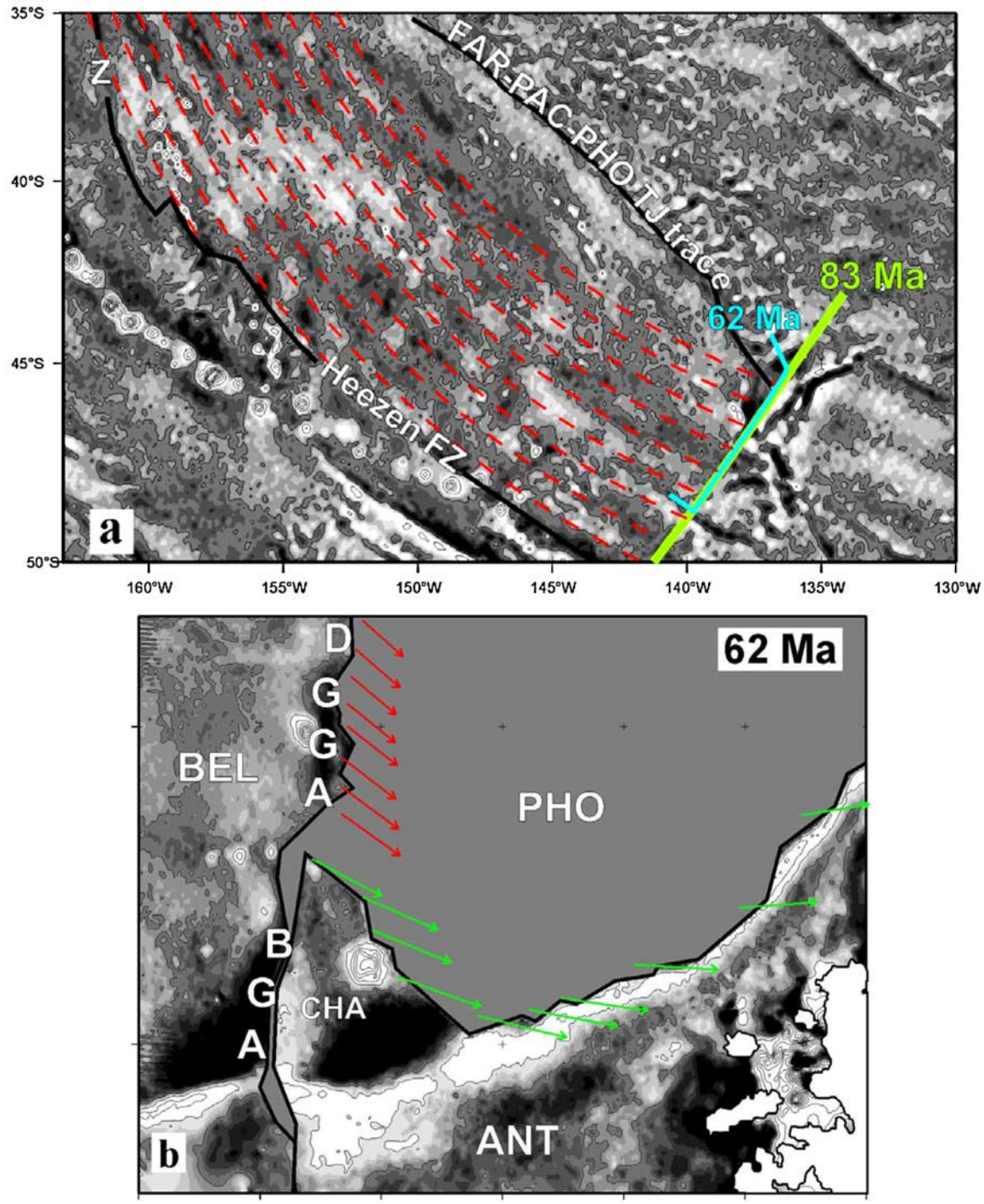

Figure 7. Estimation of relative Bellingshausen–Phoenix and Antarctic–Phoenix plate movements. (a) A Pacific–Phoenix stage pole for C34y–C27, in the Phoenix plate reference frame, is calculated by reconstructing parts of the 83 Ma (∼C34y) and 62 Ma (∼C27) Pacific plate masks (fit shown by green and blue lines, rotation of 30.15° about pole at 126.5°W, 17.2°S). Red dashed lines are segments of small circles about this stage pole, compared to free-air anomaly fabric in the area created by Pacific–Phoenix spreading during that stage. (b) Stage pole from Figure 7a used in the Pacific–Phoenix–Bellingshausen plate circuit to calculate Phoenix–Bellingshausen and Phoenix–Antarctic plate motions, for which ∼1 m.y. long vectors are shown as red and green arrows, respectively. The base map is the 62 Ma reconstruction frame with a 5° graticule interval. Mercator projections.

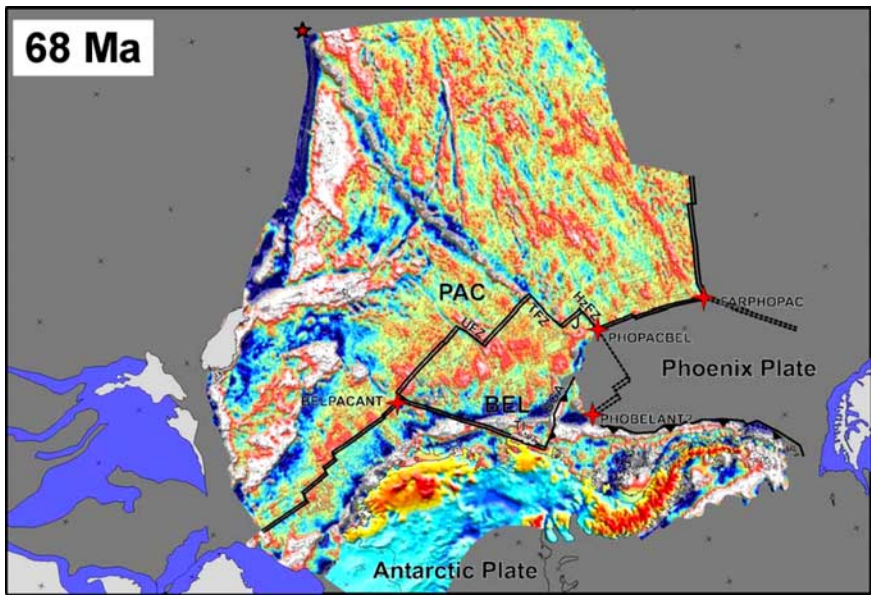

Figure 8. Animation frame for 68 Ma. Projection, graticule, symbols, and labels as for Figures 1 and 4 plus red five-point star, backtracked position of the Louisville Hot spot; J, Segment of PACBEL ridge crest that jumped to the SE at ~70 Ma.

complete by ~58 Ma (chron C26), when the full set of short-offset TFs can be seen for the first time. Similar increases have been documented from the South Atlantic [*Cande et al.*, 1988] between anomalies C30 and C20, and from the Weddell Sea [*Livermore and Hunter*, 1996] near anomaly M4. In both cases, the FZ population increases have been related to spreading rate reductions. A mantle response, involving a change from 2D to 3D mantle upwelling, has been hypothesized as the reason for this connection between decreased spreading rates and increased FZ density [*Phipps*

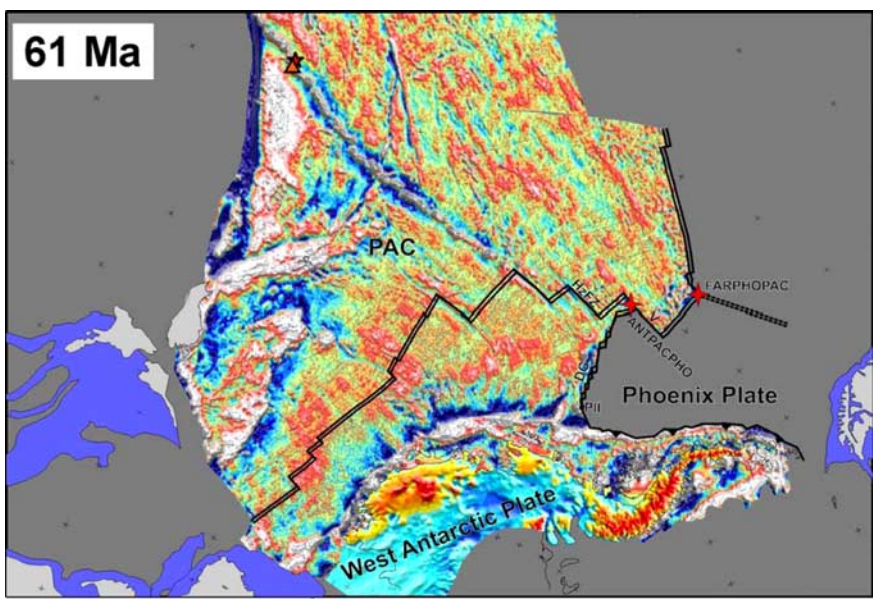

Figure 9. Animation frame for 61 Ma. Projection, graticule, symbols, and labels as for Figures 1 and 4 plus DG, De Gerlache Gravity Anomaly and De Gerlache Seamounts; orange triangle, dated sample from Louisville seamount chain (to the nearest 1 m.y. interval [*Watts et al.*, 1988]).

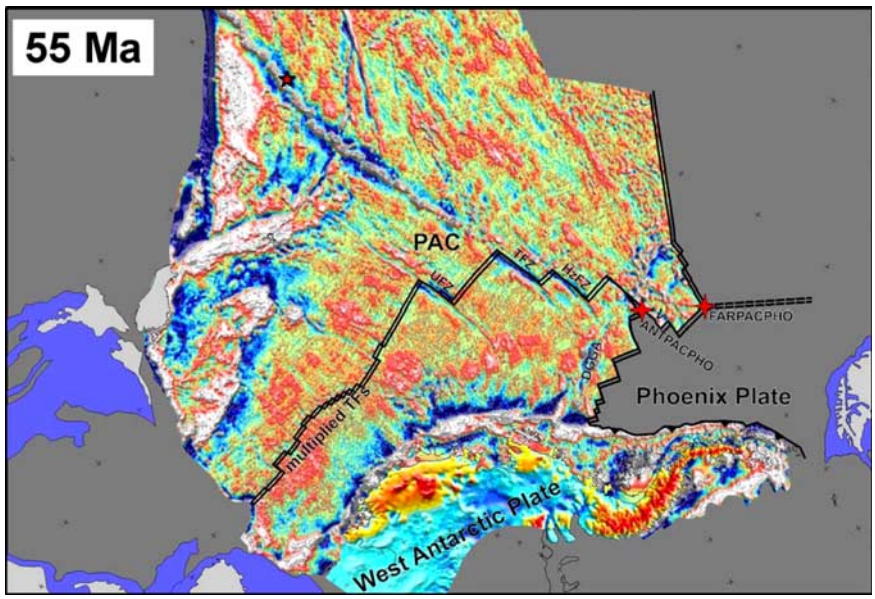

Figure 10. Animation frame for 55 Ma. Projection, graticule, symbols, and labels as for Figures 1 and 4.

Morgan and Parmentier, 1995]. If such a connection is envisaged for the South Pacific, the sudden spreading rate decrease that is visible by between chrons C27 and C25/C24 in predictions from published finite rotations may be more accurately dated to just before chron C26.

[42] The response of the Pacific–Antarctic ridge to the changes around C27 was different further north. In this frame, the amplitudes of the most recently formed parts of linear ridge-trough gravity anomalies marking the Udintsev, Tharp and Heezen TFs are markedly increased. The first appearance of the higher amplitudes along the FZs is also around anomaly C26 and appears to be independent of the different offset lengths of the TFs. Hence we think it is unlikely that the pattern is a result of differential thermal subsidence across the TFs, and suggest instead that it may be the result of transpression across these three long transforms, introduced during the rotation of Pacific–Antarctic relative motion that followed the C27 reorganization event.

3.6. Seafloor Spreading: 55-46 Ma

[43] The 46 Ma (reversed part of chron C20) frame is shown in Figure 11. The long offset Phoenix–Pacific TF on "V" no longer exists, having been bypassed by northward propagation of the Pacific–Antarctic ridge through ~15 m.y. old Pacific plate lithosphere from a starting point over 1000 km northwest of the final position of the West Antarctic–Pacific–Phoenix TJ [*Cande et al.*, 1982; *Mammerickx and Sandwell*, 1986]. This event formed a new Pacific–Antarctic spreading corridor between "V" and the Menard TF, changed the Farallon–Pacific–Phoenix TJ at the southeastern end of the Humboldt FZ to a Farallon–Antarctic–Phoenix one, and created a new Pacific–Antarctic–Farallon TJ at the Menard TF.

[44] The northward propagation of the Pacific–Antarctic ridge that formed the southern and central parts of the Henry and Hudson troughs passed through lithosphere that had formed at the Pacific–Phoenix ridge just prior to C27, and so the path of propagation may have been influenced by features that had developed in response to the C27 event. The reconstructed northern parts of the Henry and Hudson troughs are rotated by some 25°–30°, clockwise, with respect to their more southerly parts, and border anomalies C24–C21 formed between the Farallon and Pacific plates [*Cande et al.*, 1982]. Propagation here is thus likely to have exploited a Farallon–Pacific FZ. Although the active part of "V" was over 1000 km long by the time of propagation, it is tempting to speculate that the build up of stress on it was not alone enough to set off the propagation event, because propagation did not occur until the northern tip of the Antarctic–Phoenix ridge, south of "V", and the southern tip of the Pacific–Phoenix ridge, north of it, coincided, and the Pacific–Phoenix ridge south of "V"

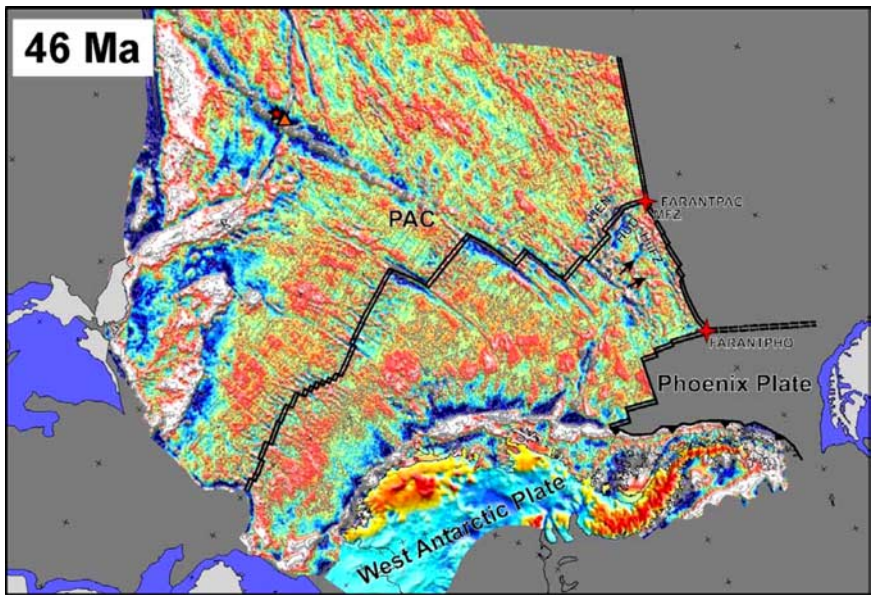

Figure 11. Animation frame for 46 Ma. Projection, graticule, symbols, and labels as for Figures 1 and 4 plus black arrows are isochron-parallel troughs in the captured crust north of "V".

was juxtaposed with Pacific plate lithosphere formed during the C27 reorganization.

[45] Isochron-parallel free-air gravity lows cross, or partially cross, the "V"–Menard corridor east of the Hudson trough, in the region of crust that was captured. *Cande* et al's [1982] profile 11 shows a double peaked magnetic anomaly C26 that coincides with the most westerly of these troughs, suggesting that some limited accretion may have occurred at it. It is possible that these features record failed westward Pacific–Phoenix ridge jumps or failed attempts to initiate a microplate in the "V"–Menard corridor, attempts to maintain "V" as active, by shortening its offset.

4. Discussion: Pre-90 Ma Events North of Chatham Rise

[46] The Hikurangi Plateau has been suggested as a conjugate feature to the ~123 Ma [*Mahoney et al.*, 1993] Manihiki Plateau Large Igneous Province that was separated from it by OT spreading, and OT has been suggested to have been part of the Pacific–Phoenix ridge that was inactivated at ~105 Ma [*Lonsdale*, 1997; *Larter et al.*, 2002]. If this was the case, it would require half spreading rates of ~90km/m.y., which are reasonable when compared to those estimated for the Pacific–Phoenix ridge in the same time period [*Larson et al.*, 2002]. However, a Manihiki-Hikurangi plateau fit would not be possible if the intervening seafloor all appeared as part of the Pacific–Phoenix ridge because it requires overall NNE-oriented relative movements, whereas Pacific–Phoenix movement was N- to NNW-oriented in the same time frame, according to abyssal hill fabric [*Larson et al.*, 2002]. However, if NNE motion had occurred, it gives an opportunity to understand gravity anomaly X other than as a long offset trench-ridge transform, whose long offset is hard to explain in the context of approach of the Charcot plate to the trench when anomaly Y already fills such a role. In fact, anomaly X is crosscut by anomaly Y at ~165.5°W, 31.6°S, and Y seems to have formed after migration of the Pacific–Phoenix ridge away from the extinct OT feature after the Hikurangi Plateau–Chatham Rise collision at ~105 Ma [*Larter et al.*, 2002]. Hence it may be that X initially formed during movements that predate Y, between the Pacific plate and another plate to the south. Specifically, X may be in part a conjugate feature to the transtensional Manihiki Scarp [*Stock et al.*, 1998] that formed after the Pacific–Phoenix ridge jumped to the Manihiki Plateau at ~119 Ma [*Larson et al.*, 2002]. A TJ between the Pacific, Phoenix and this third plate may have passed along the scarp before turning west as the Pacific–Phoenix ridge propagated west to form the ancestor to the OT. The area of seamounts between the southern end of the

Manihiki scarp and the Tonga trench at ~19°S may contain this TJ trace.

5. Summary

[47] Reconstructions made with gridded data are a way of making paleotectonic maps with detailed coverage, and relatively free of interpretation or selection by the paleocartographers, available to the geoscientific community. Animated reconstructions are powerful tools that enable presentation and discussion of paleogeography and plate tectonic histories. Our animation of reconstruction models of plate tectonic motions presents the established tectonic framework of the southern Pacific region in a widely accessible form. The animation, like any reconstruction technique, is confined to be interpreted within the constraints imposed by the starting assumptions of the animation method, and of the procedures used to derive rotation parameters, and by the data. Nonetheless, the animation allows us to illustrate events that are described in existing publications, as well as some new ones, and to connect them all as parts of the evolution of a single large ocean basin.

[48] The mid Cretaceous South Pacific margin of Gondwana was later modified by extension. A first phase of extension before chron C34y can be related to capture of part of the Phoenix plate by the Antarctic plate following collision of the Hikurangi Plateau, and the establishment of a proto Pacific–Antarctic plate margin in the Bounty Trough and Great South Basin. A second phase of Pacific–Antarctic extension, between Campbell Plateau and Marie Byrd Land, may have followed the close approach of the Charcot–Pacific ridge to this earlier margin around chron C34y, and capture of the Charcot plate by the Antarctic plate. The thus-formed mid-ocean ridge was soon afterward seeded with long offset transform faults that formed in relation to the onset and progress of independent movements of the Bellingshausen plate, itself possibly a result of the Pacific–Phoenix ridge having overtaken the Pacific–Antarctic ridge. These movements necessitated yet another extensional episode within Antarctica that may have opened Peacock Sound or other features such as Pine Island Bay between chrons C33o and C27. All of these separate Antarctic extensional plate margins may have reactivated separate lengths of a single preexisting strike-slip plate boundary or structural trend.

[49] Alongside this last extensional episode, the eastern margin of the Bellingshausen plate was shortened by up to ~200 km of convergence in the north, and by decreasing amounts further south, along a collision zone that formed by reactivation of a transform fault along the western edge of the part of the Charcot plate that had been inherited by the Antarctic plate. Around chron C27, the Bellingshausen plate ceased to have any kinematic identity, the Pacific–Antarctic plate system inherited the set of long offset transform faults from the Pacific–Bellingshausen system, and spreading changed direction and decreased in rate soon afterward. The southern sector of the Pacific–Antarctic ridge saw an increase in the number and a reversal in the offset sense of some transforms that may be related to the spreading rate decrease.

[50] The long offset transform at "V" was not simply inherited by the Pacific–Antarctic plate system around C27, because it was intersected by the northern tip of a new Antarctic–Phoenix ridge that appeared SW of it. The thus-formed Phoenix–Pacific–Antarctic triple junction migrated southeastward along the southwestern side of "V". The exact results this would have had are hard to predict because of equivocal data: but overall "V" grew ever longer while its northwestern parts were progressively transferred into the Antarctic–Phoenix system. Eventually, this complicated feature was bypassed by northeastward propagation of the Pacific–Antarctic ridge at its northwestern end. The scene was thus set for the later development of the region that was dominated by seafloor spreading at the Pacific–Antarctic and Antarctic–Phoenix ridges and the progressive subduction of the Phoenix plate beneath the Antarctic Peninsula.

Acknowledgments

[51] This project was funded by the German Research Foundation (DFG) through the grants GO 724/2-1 and GO 724/2-2. We thank Rupert Sutherland and one anonymous reviewer, as well as the numerous people who commented on earlier drafts of the animation during conference, workshop, and other presentations.

References

Barker, D. H. N., and J. A. Austin (1998), Rift propagation, detachment faulting, and associated magmatism in Bransfield Strait, Antarctic Peninsula, *J. Geophys. Res.*, *103*, 24,017–24,043.

Behrendt, J. C., W. E. LeMasurier, A. K. Cooper, F. Tessensohn, A. Trehu, and D. Damaske (1991), Geophysical studies

of the West Antarctic Rift System, *Tectonics*, *15*, 1257–1273.

Billen, M., and J. Stock (2000), Morphology and origin of the Osbourn Trough, *J. Geophys. Res.*, *105*, 13,481–13,489.

Cande, S. C., and D. V. Kent (1995), Revised calibration of the geomagnetic polarity time scale for the late Cretaceous and Cenozoic, *J. Geophys. Res.*, *100*, 6093–6096.

Cande, S. C., and J. M. Stock (2004), Cenozoic reconstructions of the Australia-New Zealand-South Pacific sector of Antarctica, in *Climate Evolution in the Southern Ocean and Australia's Cenozoic Flight North from Antarctica*, edited by N. F. Exon, M. Malone, and J. P. Kennett, AGU, Washington, D. C., in press.

Cande, S. C., E. M. Herron, and B. R. Hall (1982), The early Cenozoic tectonic history of the southeast Pacific, *Earth Planet. Sci. Lett.*, *57*, 63–74.

Cande, S. C., J. L. LaBrecque, and W. F. Haxby (1988), Plate kinematics of the South Atlantic: Chron C34 to present, *J. Geophys. Res.*, *93*, 13,479–13,492.

Cande, S. C., J. L. LaBrecque, R. L. Larson, W. C. Pitman III, X. Golovchenko, and W. F. Haxby (1989), *Magnetic Lineations of the World's Ocean Basins, Map 131*, Am. Assoc. of Pet. Geol., Tulsa, Okla.

Cande, S. C., C. A. Raymond, J. Stock, and W. F. Haxby (1995), Geophysics of the Pitman Fracture Zone and Pacific–Antarctic plate motions during the Cenozoic, *Science*, *270*, 947–953.

Cande, S. C., J. M. Stock, R. D. Müller, and T. Ishihara (2000), Cenozoic motion between East and West Antarctica, *Nature*, *404*, 145–150.

Carter, R. M. (1988), Post-breakup stratigraphy of the Kaikoura System (Cretaceous–Cenozoic), continental margin, southeastern New Zealand, *N. Z. J. Geol. Geophys.*, *31*, 405–429.

Chang, T. (1987), On the statistical properties of estimated rotations, *J. Geophys. Res.*, *92*, 6319–6329.

Cook, R. A., et al. (1999), *Cretaceous-Cenozoic Geology and Petroleum Systems of the Great South Basin, New Zealand*, *Monogr. 20*, 188 pp., Inst. of Geol. Nucl. Sci., Lower Hutt, New Zealand.

Cunningham, A. P., R. D. Larter, P. F. Barker, K. Gohl, and F. O. Nitsche (2002), Tectonic evolution of the Pacific margin of Antarctica: 2. Structure of Late Cretaceous–early Tertiary plate boundaries in the Bellingshausen Sea from seismic reflection and gravity data, *J. Geophys. Res.*, *107*(B12), 2346, doi:10.1029/2002JB001897.

Davy, B. W. (1993), The Bounty Trough—Basement structure influences on sedimentary basin evolution, in *Sedimentary Basins of the World*, vol. 2, *South Pacific Sedimentary Basins*, edited by P. F. Ballance, pp. 69–92, Elsevier Sci., New York.

Eagles, G. (2000), Modelling plate kinematics in the Scotia Sea, Ph.D. thesis, Univ. of Leeds, Leeds, U. K.

Eagles, G. (2003), Tectonic evolution of the Antarctic–Phoenix plate system since 15 Ma, *Earth Planet. Sci. Lett.*, *217*, 97–109.

Eagles, G., and R. A. Livermore (2002), Opening history of Powell Basin, Antarctic Peninsula, *Mar. Geol.*, *185*, 195–205.

Eagles, G., K. Gohl, and R. D. Larter (2004), Life of the Bellingshausen plate, *Geophys. Res. Lett.*, *31*, L07603, doi:10.1029/2003GL019127.

Gaina, C., R. D. Müller, J.-Y. Royer, J. Stock, J. Hardebeck, and P. Symonds (1998a), The tectonic history of the Tasman Sea: A puzzle with 13 pieces, *J. Geophys. Res.*, *103*, 12,413–12,433.

Gaina, C., W. Roest, and P. Symonds (1998b), The opening of the Tasman Sea: A gravity anomaly grid animation, *Earth Inter.*, *2*. (Available at http://EarthInteractions.org)

Gohl, K., F. O. Nitsche, and H. Miller (1997), Seismic and gravity data reveal Tertiary interplate subduction in the Bellingshausen Sea, southeast Pacific, *Geology*, *25*, 371–374.

Gohl, K. (Ed.) (2003), Structure and dynamics of a submarine continent: Tectonic-magmatic evolution of the Campbell Plateau (New Zealand), report of RV *SONNE* cruise SO-169, project CAMP, 17 January to 24 February 2003, *Rep. Polar Mar. Res. 457*, 88 pp., Alfred Wegener Inst., Bremerhaven, Germany.

Hagen, R. A., K. Gohl, R. Gersonde, G. Kuhn, D. Völker, and V. N. Kodagali (1998), A geophysical survey of the De Gerlache Seamounts: Preliminary results, *Geo Mar. Lett.*, *18*, 19–25.

Hall, R. (2002), Cenozoic geological and plate tectonic evolution of SE Asia and the SW Pacific: Computer-based reconstructions and animations, *J. Asian Earth. Sci.*, *20*, 353–434.

Heinemann, J., J. Stock, K. Clayton, S. Hafner, S. Cande, and C. Raymond (1999), Constraints on the proposed Marie-Byrd Land–Bellingshausen plate boundary from seismic reflection data, *J. Geophys. Res.*, *104*, 25,321–25,330.

Hellinger, S. J. (1981), The uncertainties of finite rotations in plate tectonics, *J. Geophys. Res.*, *86*, 9312–9318.

Larson, R. L., R. A. Pockalny, R. F. Viso, E. Erba, L. J. Abrams, B. P. Luyendyk, J. M. Stock, and R. W. Clayton (2002), Mid-Cretaceous tectonic evolution of the Tongareva triple junction in the southwestern Pacific Basin, *Geology*, *30*, 67–70.

Larter, R. D., and P. F. Barker (1991), Effects of ridge-crest–trench interaction on Antarctic-Phoenix spreading: Forces on a young subducting plate, *J. Geophys. Res.*, *96*, 19,583–19,607.

Larter, R. D., A. P. Cunningham, P. F. Barker, K. Gohl, and F. O. Nitsche (1999), Structure and tectonic evolution of the West Antarctic continental margin and Bellingshausen Sea, *Korean J. Polar Res.*, *10*, 125–133.

Larter, R. D., A. P. Cunningham, P. F. Barker, K. Gohl, and F. O. Nitsche (2002), Tectonic evolution of the Pacific margin of Antarctica: 1. Late Cretaceous tectonic reconstructions, *J. Geophys. Res.*, *107*(B12), 2345, doi:10.1029/2000JB000052.

Livermore, R. A., and R. J. Hunter (1996), Mesozoic seafloor spreading in the southern Weddell Sea, in *Weddell Sea Tec-*

tonics and Gondwana Break-up, edited by B. C. Storey, E. C. King, and R. A. Livermore, *Geol. Soc. Spec. Publ.*, *108*, 227–241.

Livermore, R. A., et al. (2000), Autopsy on a dead spreading center: The Phoenix Ridge, Drake Passage, Antarctica, *Geology*, *28*, 607–610.

Lonsdale, P. (1997), An incomplete geologic history of the southwest Pacific basin, *Geol. Soc. Am. Abstr. Programs*, *29*, 4574.

Luyendyk, B. P. (1995), Hypothesis for Cretaceous rifting of east Gondwana caused by subducted slab capture, *Geology*, *23*, 373–376.

Lythe, M. B., D. G. Vaughan, and the BEDMAP Consortium (2000), BEDMAP—Bed topography of the Antarctic, scale 1:10,000,000, Br. Antarct. Surv., Cambridge, U. K.

Mahoney, J. J., M. Storey, R. A. Duncan, K. J. Spencer, and M. Pringle (1993), Geochemistry and age of the Ontong Java Plateau, in *The Mesozoic Pacific: Geology, Tectonics and Volcanism*, *Geophys. Monogr. Ser.*, vol. 77, edited by M. S. Pringle et al., pp. 233–261, AGU, Washington, D. C.

Mammerickx, J., and D. Sandwell (1986), Rifting of old oceanic lithosphere, *J. Geophys. Res.*, *91*, 1975–1988.

Marks, K. M., and J. M. Stock (1997), Early Tertiary gravity field reconstructions of the Southwest Pacific, *Earth Planet. Sci. Lett.*, *152*, 267–274.

Mayes, C. L., L. A. Lawver, and D. T. Sandwell (1990), Tectonic history and new isochron chart of the South Pacific, *J. Geophys. Res.*, *95*, 8543–8567.

McAdoo, D. C., and S. Laxon (1997), Antarctic tectonics: Constraints from an ERS-1 satellite marine gravity field, *Science*, *276*, 556–560.

McCarron, J. J., and R. D. Larter (1998), Late Cretaceous to early Tertiary subduction history of the Antarctic Peninsula, *J. Geol. Soc. London*, *155*, 255–268.

Mitchell, N. C., and L. M. Parson (1993), The tectonic evolution of the Indian Ocean Triple Junction, anomaly 6 to present, *J. Geophys. Res.*, *98*, 1793–1812.

Mortimer, N., and D. Parkinson (1996), Hikurangi Plateau: A Cretaceous large igneous province in the southwest Pacific, *J. Geophys. Res.*, *101*, 687–696.

Müller, R. D., and W. R. Roest (1992), FZs in the North Atlantic from combined Geosat and Seasat data, *J. Geophys. Res.*, *97*, 3337–3350.

Müller, R. D., C. Gaina, A. Tikku, D. Mihut, S. C. Cande, and J. M. Stock (2000), Mesozoic/Cenozoic tectonic events around Australia, in *The History and Dynamics of Global Plate Motions*, *Geophys. Monogr. Ser.*, vol. 121, pp. 161–188, AGU, Washington, D. C.

Nankivell, A. P. (1997), Tectonic history of the Southern Ocean since 83 Ma, Ph.D. thesis, Oxford Univ., Oxford, U. K.

Phipps Morgan, J., and E. M. Parmentier (1995), Crenulated seafloor: Evidence for spreading-rate dependent structure of mantle upwelling and melting beneath a mid-oceanic spreading centre, *Earth Planet. Sci. Lett.*, *129*, 73–84.

Prestvik, T., and R. A. Duncan (1991), The geology and age of Peter I Øy, Antarctica, *Polar Res.*, *9*, 89–98.

Reeves, C., and B. K. Sahu (1999), Computer animation of Gondwana dispersal and the history of igneous extrusion in the Indian Ocean, paper presented at IUGG99, Int. Union of Geod. and Geophys., Birmingham, U. K.

Royer, J.-Y., and N. Rollet (1997), Plate-tectonic setting of the Tasmanian region, in *West Tasmanian Margin and Offshore Plateaus: Geology, Tectonic and Climatic History, and Resource Potential*, edited by N. F. Exon, and A. J. Crawford, *Aust. J. Earth Sci.*, *44*, 543–560.

Sandwell, D. T., and W. H. F. Smith (1997), Marine gravity anomaly from Geosat and ERS 1 satellite altimetry, *J. Geophys. Res.*, *102*, 10,039–10,054.

Shaw, P. R., and S. C. Cande (1990), High resolution inversion for South Atlantic plate kinematics using joint altimeter and magnetic anomaly data, *J. Geophys. Res.*, *95*, 2625–2644.

Stock, J. M., and P. Molnar (1987), Revised early Tertiary history of plate motions in the southwest Pacific, *Nature*, *325*, 495–499.

Stock, J. M., S. C. Cande, and C. A. Raymond (1996), Updated history of the Bellingshausen Plate, *Eos Trans. AGU*, *77*, Fall Meet. Suppl., F647.

Stock, J. M., B. P. Luyendyk, R. W. Clayton, and Shipboard Scientific Party (1998), Tectonics and structure of the Manihiki Plateau, western Pacific Ocean, *Eos Trans. AGU*, *79*, Fall Meet. Suppl., F870.

Sutherland, R. (1995), The Australia-Pacific boundary and Cenozoic plate motions in the SW Pacific: Some constraints from Geosat data, *Tectonics*, *14*, 819–831.

Sutherland, R. (1999), Basement geology and tectonic development of the greater New Zealand region: An interpretation from regional magnetic data, *Tectonophysics*, *308*, 341–362.

Thomas, T., R. A. Livermore, and F. Pollitz (2003), Motion of the Scotia Sea plates, *Geophys. J. Int.*, *155*, 789–804.

Tikku, A., and S. C. Cande (2000), On the fit of Broken Ridge and Kerguelen plateau, *Earth Planet. Sci. Lett.*, *180*, 117–132.

Watts, A. B., J. K. Weissel, R. A. Duncan, and R. L. Larson (1988), Origin of the Louisville Ridge and its relationship to the Eltanin Fracture Zone System, *J. Geophys. Res.*, *93*, 3051–3077.

Wessel, P., and L. Kroenke (1997), A geometric technique for relocating hotspots and refining absolute plate motions, *Nature*, *387*, 365–369.

Wessel, P., and W. H. F. Smith (1998), New, improved version of Generic Mapping Tools released, *Eos Trans. AGU*, *79*, 579.

Wood, R., R. Herzer, R. Sutherland, and A. Melhuish (2000), Cretaceous-Tertiary tectonic history of the Fiordland margin, New Zealand, *N. Z. J. Geol. Geophys.*, *43*, 289–302.

Yan, C.-Y., and L. W. Kroenke (1993), A plate tectonic reconstruction of the southwest Pacific, 0–100 Ma, *Proc. Ocean Drill. Program Sci. Results*, *130*, 697–709.